J|A|C|S
COMMUNICATIONS

Published on Web 07/29/2006

Detection of Peptide−Phospholipid Interaction Sites in Bilayer Membranes by ^{13}C NMR Spectroscopy: Observation of $^{2}H/^{31}P$-Selective ^{1}H-Depolarization under Magic-Angle Spinning

Erisa Harada,[†,‡] Yasuto Todokoro,[†] Hideo Akutsu,[†] and Toshimichi Fujiwara*[,†]

Institute for Protein Research, Osaka University, Suita, 565-0871, Japan, and Japan Biological Informatics Consortium, Chuo-ku, Tokyo, 104-0032, Japan

Received April 21, 2006; E-mail: tfjwr@protein.osaka-u.ac.jp

Interactions between phospholipids and proteins/peptides govern the structure of functionally important membrane proteins. Several spectroscopic and diffraction methods are available for studying the interaction,[1−5] but it is still difficult to elucidate the structure of the protein−membrane systems. Solid-state NMR is a powerful method for the structural analysis of proteins interacting with lipid bilayer membranes. Solid-state NMR for uniaxially oriented proteins provides angular constraints with respect to the membrane normal.[6] Distance information for protein−membrane systems can be obtained from $^{31}P-^{13}C$ dipolar couplings for selectively isotope-labeled peptides[7] and from ^{1}H spin diffusion.[8] Paramagnetic probes also provide the structural information.[9]

We propose a novel method for probing intermolecular interfaces by magic-angle spinning solid-state NMR.[10,11] This method gives ^{13}C NMR spectra for the distance correlation between ^{1}H spins in a peptide and $^{2}H/^{31}P$ spins in lipids. We have applied this method to a membrane system consisting of a uniformly ^{13}C-, ^{15}N-labeled peptide mastoparan-X (MP-X) and phospholipids having perdeuterated acyl chains. This 14-residue peptide, MP-X, has an amphiphilic helix and activates G-proteins.[12−15] Under our experimental conditions, MP-X tightly binds to the anionic lipid bilayers used but does not disrupt the bilayer structure.[16]

The pulse sequence for obtaining ^{13}C NMR spectra that provide the ^{1}H-depolarization-mediated $^{31}P-^{1}H$ and $^{2}H-^{1}H$ distance correlation is shown in Figure 1. The initial pulses prepare the X (^{31}P or ^{2}H) and ^{1}H magnetization spin-locked parallel and antiparallel to the effective fields in the rotating frames, respectively. The ^{1}H magnetization is depolarized by $^{1}H-X$ dipolar interactions recoupled under a sideband Hartmann−Hahn condition. Proton spin diffusion during the depolarization is suppressed by the ^{1}H effective field at the magic angle.[17] After the spin system reaches a quasi-equilibrium state, the X magnetization transferred from ^{1}H is effectively inverted with respect to the B_1 field for X by alternating the B_1 phase. The inversion makes the system nonequilibrium and allows further ^{1}H depolarization.[18,19] This inversion is iterated so as to maximize the ^{1}H depolarization by $X-^{1}H$ dipolar couplings. The subsequent Lee−Goldburg cross polarization (LGCP) transfers the ^{1}H magnetization to the attached ^{13}C spins. Thus, the ^{1}H depolarization is monitored through high-resolution ^{13}C NMR spectra. This method, ^{13}C observation of X-selective ^{1}H-depolarization (COXSHD), provides $^{1}H-X$ distance information from the heteronuclear dipolar couplings.

Spectra for the ^{2}H- and ^{31}P-selective ^{1}H-depolarization of MP-X are shown in Figure 2. Because they are the differences between spectra obtained under on and off Hartmann−Hahn conditions for the depolarization, the signal intensities indicate the magnitudes

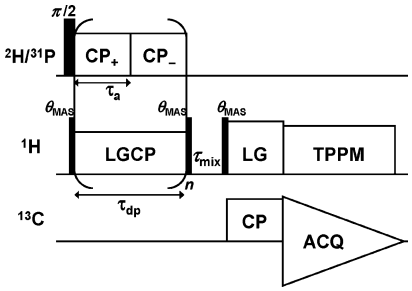

Figure 1. Pulse sequence for ^{13}C-observation of X-selective ^{1}H-depolarization under MAS. The RF phase for the depolarization period was alternated at the intervals of $\tau_a = 240$ and 160 μs for ^{2}H and ^{31}P, respectively. The ^{1}H depolarization is facilitated by the phase-alternating cross polarization. The flip angles of all the ^{1}H pulses are 54.7°. The B_1 field amplitudes satisfy the condition $\gamma B_{1,X} = \gamma B_{1,1H}^{eff} - \omega_R$ at the spinning rate $\omega_R/2\pi$ of 12.5 kHz and the $B_{1,X}$ amplitude of 31 kHz for ^{2}H and 52 kHz for ^{31}P. The frequency of $B_{1,X}$ was shifted by about 130 kHz under the off Hartmann−Hahn condition. Contact time for $^{13}C-^{1}H$ LGCP was 80 μs.

of the depolarization of ^{1}H spins in MP-X. The spectra for the ^{2}H-selective and ^{31}P-selective depolarization, respectively, reveal the ^{1}H spins in the vicinity of ^{2}H in the fatty acyl chains and of ^{31}P in the hydrophilic headgroups. The spectral patterns for the depolarization (Figure 2 a,b) are different from the reference spectrum (Figure 2c). The backbone structure and ^{13}C chemical shifts of membrane-bound MP-X were previously determined by our solid-state NMR study.[12] This enables the assignment of the $^{13}C^{\alpha}$ signals for the ^{2}H-selective depolarization to the spins in hydrophobic residues, Ile, Leu, and Ala, as shown in Figure 2. The strong indole ring signals resonating at about 120 ppm indicate that the ring contacted the hydrophobic acyl chains. The $^{13}C^{\alpha}$ depolarization spectrum for ^{31}P exhibits large signal intensities for hydrophilic side chains such as Lys in addition to hydrophobic residues. Indole ring signals observed in the $CO^{31}PSHD$ spectrum indicate that the ring interacted with ^{31}P atoms in the interface region in addition to acyl chains in lipids.[20]

We have determined the position and orientation of MP-X in the lipid bilayers by simulating the depolarization spectra. This simulation was based on the ^{1}H-depolarization intensity profile as a function of the membrane depth z shown in Figure 3a. This z dependence was calculated for the distribution of ^{2}H and ^{31}P atoms in a DPPC bilayer generated by a molecular dynamics simulation[21] (see Supporting Information for details). The depolarization spectra for the C^{α} spins were calculated for a series of structures as a function of the depth z and the orientation of the helix. The minimum RMSD between the experimental and simulated depolarization spectra for ^{2}H and ^{31}P was obtained by the structure shown in Figure 3a. The calculated spectra are shown in Figure 2a,b by broken lines. Signal assignments based on this structure are also given. Correlations of the $^{1}H^{\alpha}$ spins with ^{31}P and ^{2}H spins in lipids

[†] Osaka University.
[‡] Japan Biological Information Consortium.

10.1021/ja062811u CCC: $33.50

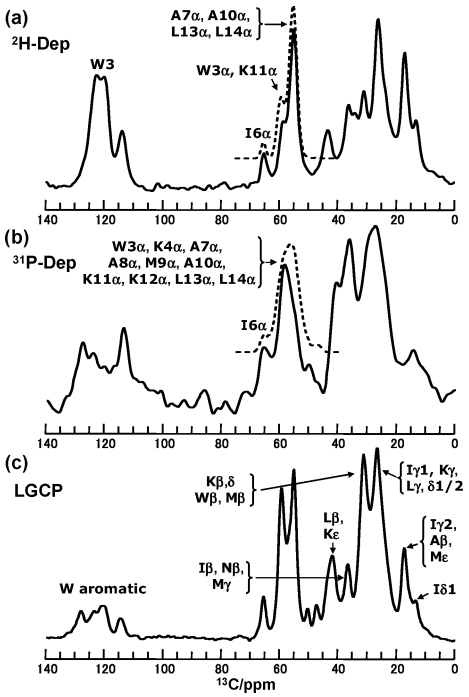

Figure 2. (a) ^{13}C difference spectrum for the ^{2}H-selective ^{1}H-depolarization of membrane-bound MP-X at $\tau_{dp} = 2.88$ ms. (b) ^{13}C difference spectrum for the ^{31}P-selective depolarization at $\tau_{dp} = 0.96$ ms. Best-fit spectra simulated from the structure model are show by broken lines. (c) ^{13}C spectrum obtained with LGCP. All the experiments were made at the ^{1}H frequency of 499.9 MHz under −50 °C and relative humidity of 32% for a mixture of MP-X and liposomes consisting of DMPC and DMPG (4:1) with a lipids/MP-X molar ratio of 20. The number of transients was 16 000 (a), 35 200 (b), and 32 (c).

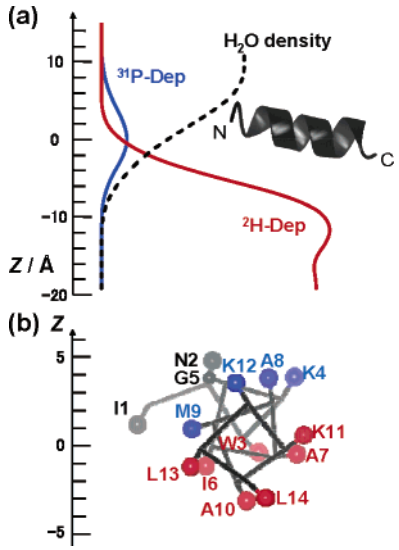

Figure 3. (a) ^{2}H- and ^{31}P-selective ^{1}H-depolarization as a function of the depth z from the level giving the largest ^{31}P density in lipid bilayers. The depths of H^{α} atoms in MP-X shown in the figure give the best fit simulation spectra in Figure 2a,b. Water density is shown by a broken line. (b) Helix wheel diagram representation of MP-X (a) viewed from the C-terminus. The correlation between phospholipids and $^{1}H^{\alpha}$ in amino acid residues is shown. Strong correlations of $^{1}H^{\alpha}$ with ^{2}H and ^{31}P spins are indicated by color-coded C^{β} balls: blue for ^{31}P and red for ^{2}H and ^{31}P. Precisions for the depth z, the rotation angle about the helix axis, and the helix tilt angle about the axis in the membrane plane and perpendicular to the helix axis were ±1.2 Å, ±12°, and ±4°, respectively. The bilayer center is at $z = -19.2$ Å.

are mapped on the helix wheel diagram in Figure 3b. This figure indicates that MP-X is located in the interface between the water layer and hydrophobic domain of lipid bilayers with nonpolar residues facing the phosphorus atoms and alkyl chains of the lipids.

We have shown that ^{13}C spectra for the X-selective ^{1}H-depolarization provide the distance correlation from dipolar couplings between ^{1}H in peptides and ^{31}P and ^{2}H in lipids. This method has advantages: (1) Use of a large γ nucleus, ^{1}H, allows obtaining the distances from strong dipolar couplings as shown in REDOR for ^{1}H spins.[22] (2) The distance information for the dipolar couplings are obtained through all the ^{13}C spins in the labeled peptide, which can be observed under the high-resolution condition. (3) Experiments with the sequence in Figure 1 provide sensitivities higher than ^{1}H-mediated X−^{13}C magnetization transfer because of accumulated ^{1}H-depolarization by the multiple-contact cross-polarization, as shown in Supporting Information. (4) A single sample, uniformly ^{13}C-labeled peptide and deuterated lipid can be used for the interacting sites analysis as well as for the peptide structure determination.

Acknowledgment. This work was partly supported by Strategic International Cooperative Program. We appreciate Ms. I. Yumen, Prof. K. Wakamatsu, and Dr. T. Kohno for the sample preparation.

Supporting Information Available: Parameters for the pulse sequence, time-dependence of the depolarization, and calculation of the ^{13}C spectral intensities. This material is available free of charge via the Internet at http://pubs.acs.org.

References

(1) Gonen, T.; Cheng, Y.; Sliz, P.; Hiroaki, Y.; Fujiyoshi, Y.; Harrison, S. C.; Walz, T. *Nature* **2005**, *438*, 633−638.
(2) Tucker, M. J.; Getahun, Z.; Nanda, V.; DeGrado, W. F.; Gai, F. *J. Am. Chem. Soc.* **2004**, *126*, 5078−5079.
(3) Nakamura, T.; Takahashi, H.; Takeuchi, K.; Kohno, T.; Wakamatsu, K.; Shimada, I. *Biophys. J.* **2005**, *89*, 4051−4055.
(4) Egashira, M.; Gorbenko, G.; Tanaka, M.; Saito, H.; Molotkovsky, J.; Nakano, M.; Handa, T. *Biochemistry* **2002**, *41*, 4165−4172.
(5) Fanucci, G. E.; Cadieux, N.; Piedmont, C. A.; Kadner, R. J.; Cafiso, D. S. *Biochemistry* **2002**, *41*, 11543−11551.
(6) Opella, S. J.; Marassi, F. M. *Chem. Rev.* **2004**, *104*, 3587−3606.
(7) Toke, O.; Maloy, L. W.; Kim, S. J.; Blazyk J.; Schaefer, J. *Biophys. J.* **2004**, *87*, 662−674.
(8) Gallagher, G. J.; Hong, M.; Thompson, L. K. *Biochemistry* **2004**, *43*, 7899−7906.
(9) Grobner, G.; Glaubitz, C.; Watts, A. *J. Magn. Reson.* **1999**, *141*, 335−339.
(10) Kiihne, S. R.; Creemers A. F. L.; de Grip, W. J.; Bovee-Geurts P. H. M.; Lugtenburg, J.; de Groot, H. J. M. *J. Am. Chem. Soc.* **2005**, *127*, 5734−5735.
(11) Etzkorn, M.; Böckmann, A.; Lange, A.; Baldus, M. *J. Am. Chem. Soc.* **2004**, *126*, 14746−12751.
(12) Todokoro, Y.; Yumen, I.; Fukushima, K.; Kang, S.-W.; Park, J.-S.; Kohno, T.; Wakamatsu, K.; Akutsu, H.; Fujiwara, T. *Biophys. J.* **2006**, *91*, 1368−1379.
(13) Fujiwara, T.; Todokoro, Y.; Yanagishita, H.; Tawarayama, M.; Kohno, T.; Wakamatsu, K.; Akutsu, H. *J. Biomol. NMR* **2004**, *28*, 311−325.
(14) Whiles, J. A.; Brasseur, R.; Glover, K. J.; Melacini, G.; Komives, E. A.; Vold, R. R. *Biophys. J.* **2001**, *80*, 280−293.
(15) Wakamatsu, K.; Okada, A.; Miyazawa, T.; Ohya, M.; Higashijima, T. *Biochemistry* **1992**, *31*, 5654−5660.
(16) Matsuzaki, K.; Yoneyama, S.; Murase, O.; Miyajima, K. *Biochemistry* **1996**, *35*, 8450−8456.
(17) Ladizhansky, V.; Vega, S. *J. Chem. Phys.* **2000**, *112*, 7158−7168.
(18) Zumbulyadis, N. *J. Chem. Phys.* **1987**, *86*, 1162−1166.
(19) Shnha, N.; Ramanathan, K. V. *Chem. Phys. Lett.* **2000**, *332*, 125−130.
(20) Killian, J. A. *Biochim. Biophys. Acta* **1998**, *1376*, 401−416.
(21) Feller, S. E.; Venable, R. M.; Pastor, R. W. *Langmuir* **1997**, *13*, 6555−6561.
(22) Wi, S.; Sinha, N.; Hong, M. *J. Am. Chem. Soc.* **2004**, *126*, 12754−12755.

JA062811U